EUR 337.e

DEVELOPMENT OF METHODS FOR THE DETERMINATION OF THE HIGH TEMPERATURE THERMAL DIFFUSIVITY OF UC

by

C. MUSTACCHI and S. GIULIANI

1963

DEVELOPMENT OF METHODS FOR THE DETERMINATION OF THE HIGH TEMPERATURE THERMAL DIFFUSIVITY OF UC
by C. MUSTACCHI and S. GIULIANI

European Atomic Energy Community — EURATOM
Joint Nuclear Research Center
Ispra Establishment (Italy)
Materials Department — Physical Chemistry Service
Brussels, August 1963, pages 27 + figures 11.

A simple modulated electron gun is used to determine the thermal diffusivity of uranium carbide in the range 1000° to 2000 °C. Both a sine wave and a pulse techniques are applied to thin wafer shaped samples of carbide. Temperature of the hind face is detected by means of a photocell-oscilloscope arrangement. Arc-cast carbide yielded a value .049± .004 cm² sec⁻¹ for thermal diffusivity in the range in question.
Values for emissivity, electrical and thermal conductivity were measured or derived for uranium carbide.

EUR 337.e

EUROPEAN ATOMIC ENERGY COMMUNITY — EURATOM

DEVELOPMENT OF METHODS FOR THE DETERMINATION OF THE HIGH TEMPERATURE THERMAL DIFFUSIVITY OF UC

by

C. MUSTACCHI and S. GIULIANI

1963

INDEX

DEVELOPMENT OF METHODS FOR THE DETERMINATION
OF THE HIGH TEMPERATURE THERMAL DIFFUSIVITY OF UC

SUMMARY

A simple modulated electron gun is used to determine the thermal diffusivity of uranium carbide in the range 1000° to 2000 °C. Both a sine wave and a pulse techniques are applied to thin wafer shaped samples of carbide. Temperature of the hind face is detected by means of a photocell-oscilloscope arrangement. Arc-cast carbide yielded a value .049± .004 cm^2 sec^{-1} for thermal diffusivity in the range in question.

Values for emissivity, electrical and thermal conductivity were measured or derived for uranium carbide.

1 — SCOPE OF THE RESEARCH

As a first step in a comprehensive research program to investigate gap or contact conductance between a UC fuel pellet and metal clad, it was felt necessary to determine the UC thermal conductivity in the full range of temperatures encountered in an operating reactor.

Preliminary data on fission gas release from sintered and fused UC pointed out to operating temperatures as high as 1600 °C with fairly substantial retention of said gases.

However, no measurements of thermal properties of UC are available beyond 800 °C [1]. Further, no reliable method is known for extrapolating thermal conductivity of UC to high temperatures.

These facts led us to aim at the development of methods suitable for a quick determination of ceramic fuels conductivity in the range 1000 to 2000 °C.

2 — HIGH TEMPERATURE CONDUCTIVITY MECHANISMS

In order to evaluate the uncertainties in the extrapolation of low temperature data, a simple analysis of the contribution of different phenomena to heat transport in UC is given hereafter.

The three main mechanisms of heat transport through solids are :

a) migration of electrons or holes
b) lattice vibrations propagation
c) transparency of electromagnetic radiation.

The contribution of mechanism a) can be estimated by means of the Wiedemann-Franz relation

$$\frac{K_1}{T} = 2 K^2/e^2$$

where ϱ = electrical resistivity
T = temperature, degrees Kelvin
K_1 = thermal conductivity
K = Boltzmann constant
e = electronic charge

Assuming a value $\mu = 4 \times 10^{-5}$ ohm/cm at 100 °C [2,3], the electron contribution to thermal conductivity is of the order of 0,14 W/cm °C. Since resistivity in the range 100 to 800 °C

5

is reported to increase linearly with temperature, it may be expected that K_1 at 800 °C will be but little different than at 100 °C. This means that at least in the range 100 to 800 °C [4] the contribution of mechanism a) is but little affected by temperature and ranges from 50 to 60% of overall thermal conductivity [1].

As to mechanism b), its contribution is [5] :

$$K_2 = \frac{3Klv}{C^2}$$

where l is the phonon mean free path

v = sound velocity

C = lattice constant

With high impurity levels, l approaches C. Call $l = nC$ to measure the mean free path in lattice parameter units

$$K_2 = \frac{3Kvn}{C^2}.$$

With a modulus of elasticity $222\ 10^6$ kg/cm² [1] and a density $d = 13,6$, the velocity of sound is

$$v = \frac{X \cdot g}{d} = 4.000 \text{ m/sec.}$$

With a lattice constant $C = 5$ Å [6] $= 5 \times 10^{-10}$ m

$$K_2 = \frac{3 \times 1,4 \times 10^{-23} \times 4,000\,n}{(5 \times 10^{-10})^2} = 67\,n\,\frac{w}{°C \times m} = .0067\,n\,\frac{w}{°C \times cm}.$$

It may be expected [7] that n decreases from, say 20 at ambient temperature to a value of 2 or 3 at temperatures in excess of 1000 °K.

The lattice contribution to thermal conductivity would then be about .13 w/°C cm at 100 °C and .02 w/°C × cm at 1000 °K.

By summing the contributions of mechanism a) and b), we can account for the whole thermal conductivity at ambient temperature, i.e.

$$K = K_1 + K_2 = .14 + .13 = .27 \text{ } w/cm\,°C$$

and we might expect a conductivity at 1500 °K.

$$K = .14 + .02 = .16 \text{ } w/cm\,°C.$$

At higher temperatures, we must, however, take into consideration mechanism c). To evaluate an order of magnitude for this mechanism, we can use a simplified Genzel model [8] as proposed by earlier workers [8,10]. In this model, radiation has an average absorption coefficient characteristic of the transparent regions of the infrared spectrum, say $a = .1$ cm⁻¹.

A photon undergoes a random walk with a scattering process at each crystallite boundary. The effective mean free path is given by [9]

$$a' = (a/d)^{1/2}$$

where d is the mean diameter of the crystallites.

The contribution to heat transport will be

$$K_3 = \frac{16}{3} \quad T^3 \frac{\bar{n}^2}{a'}$$

where $\bar{n}$ is some suitable mean refraction index.

6

In the case of our UC sample $d = 10^{-2}$ cm (see fig. 1) therefore $a' = 3,2^\circ$.
Assuming $n = 1.5$ $K_3 = .02$ at $1000^\circ K$ and $.16$ w/cm° at $2000^\circ K$.

Fig. 1 — Uranium Carbide 100 ×

These orders of magnitude show that mechanism c) is likely to have a negligible contribution below $1000^\circ K$ but that it may be of the same order as the electronic conductivity at $2000^\circ K$.

3 — CHOICE OF A METHOD

In order to select a method best adapted to the problem on hand, we had to meet the following specifications :

a) Small amounts ($<$ 5 g) of material must be sufficient to enable one to handle reasonable amounts of activity in the case of irradiated UC.

b) Measurements must be performed in a high vacuum, because of the high chemical reactivity of UC in the range of temperature 1000-2000°K.

c) Direct temperature measurements and the use of thermocouples have to be avoided as far as possible, since no material is reportedly compatible with UC beyond 1500°K, at least as far as relying upon failsafe thermocouple performance.

Because of end effects in small samples and the necessity of using thermocouples, spec. ([1]) and ([3]) rule out any steady state method, be it longitudinal or radial.

We are left with a choice among the several transient methods consisting in an analysis of the transfer function, temperature vs. power input in a sample.

This power input function can be a sine wave, a square wave or a pulse.

As for temperature measurements we chose an optical method using a photoconductive cell as a sensing device and for heating, after examining the possibility of using an arc image furnace, a laser flashhead or a high frequency generator (induction furnace), we finally selected an electron gun system on account of the relative ease of modulating the power input.

As far as the geometry of the sample is concerned, two shapes were investigated : the hollow cylinder and the thin wafer. The transfer functions for both cases are given in Appendices I and II.

Calculation and plots made with the help of the Ispra IBM 7090 computer showed that a better sensitivity was to be expected in the wafer geometry. Further, this geometry leads to simpler sample preparation and electron gun design.

Summarizing the specifications :

— UC wafers are 1 to 3 mm thick and about 12 mm dia.

— Electron gun heating is performed in a vacuum better than 10^{-5} mm Hg.

— Modulation of power input is obtained by control of the electron beam, thus allowing a wide range of input wave forms.

— A photoresistive cell is used to measure temperature variations.

4 — EXPERIMENTAL SETUP

The scheme of the apparatus is given in fig. 2 and its overall setup in fig. 3.

4.1 — Electron gun

Following Pierce's advice (*), a trial-and-error construction was made. After a number of changes the gun attained a relative peak of selection and looked somewhat as shown in fig. 4 and 5.

(*) J.R. Pierce : "Theory and Design of Electron Beams", Second Edition, p. 215 : "If one wishes to spray a surface with a weak electron beam it is usually foolish to design a gun to do this. A tungsten filament and an accelerating grid or apertured plate will do well enough."
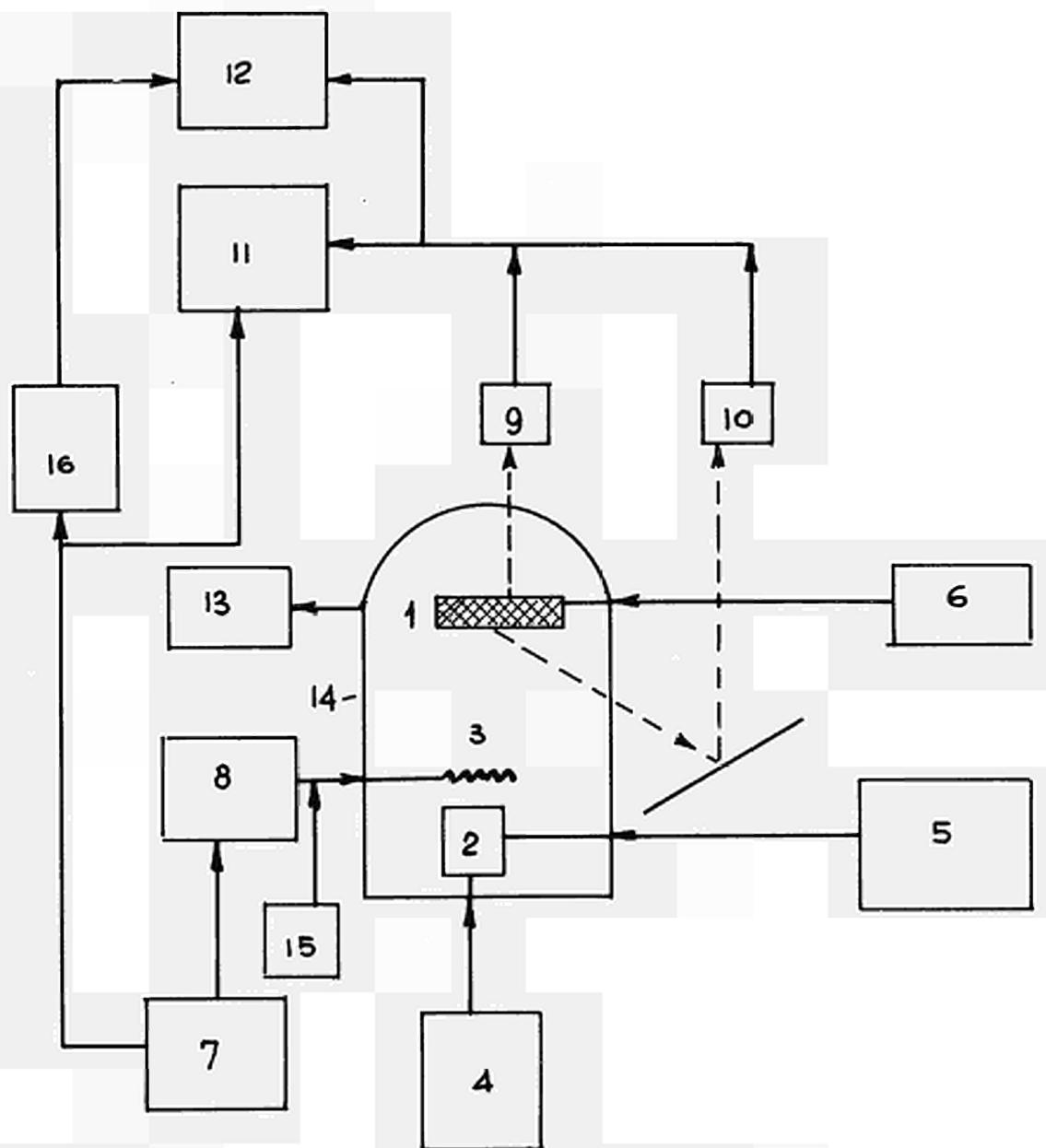
Fig. 2 — Experimental setup

1. Sample wafer
2. Electron gun
3. Modulating electrode
4. Filament power supply
5. Electrostatic lens supply
6. Accelerating voltage supply
7. Wave function generator
8. Balanced variable amplier

9-10. Phototube detectors
11. Phase analyzer
12. Oscilloscope or recorder
13. Vacuum pumps
14. Vacuum jar
15. Grid bias supply
16. Delay circuit
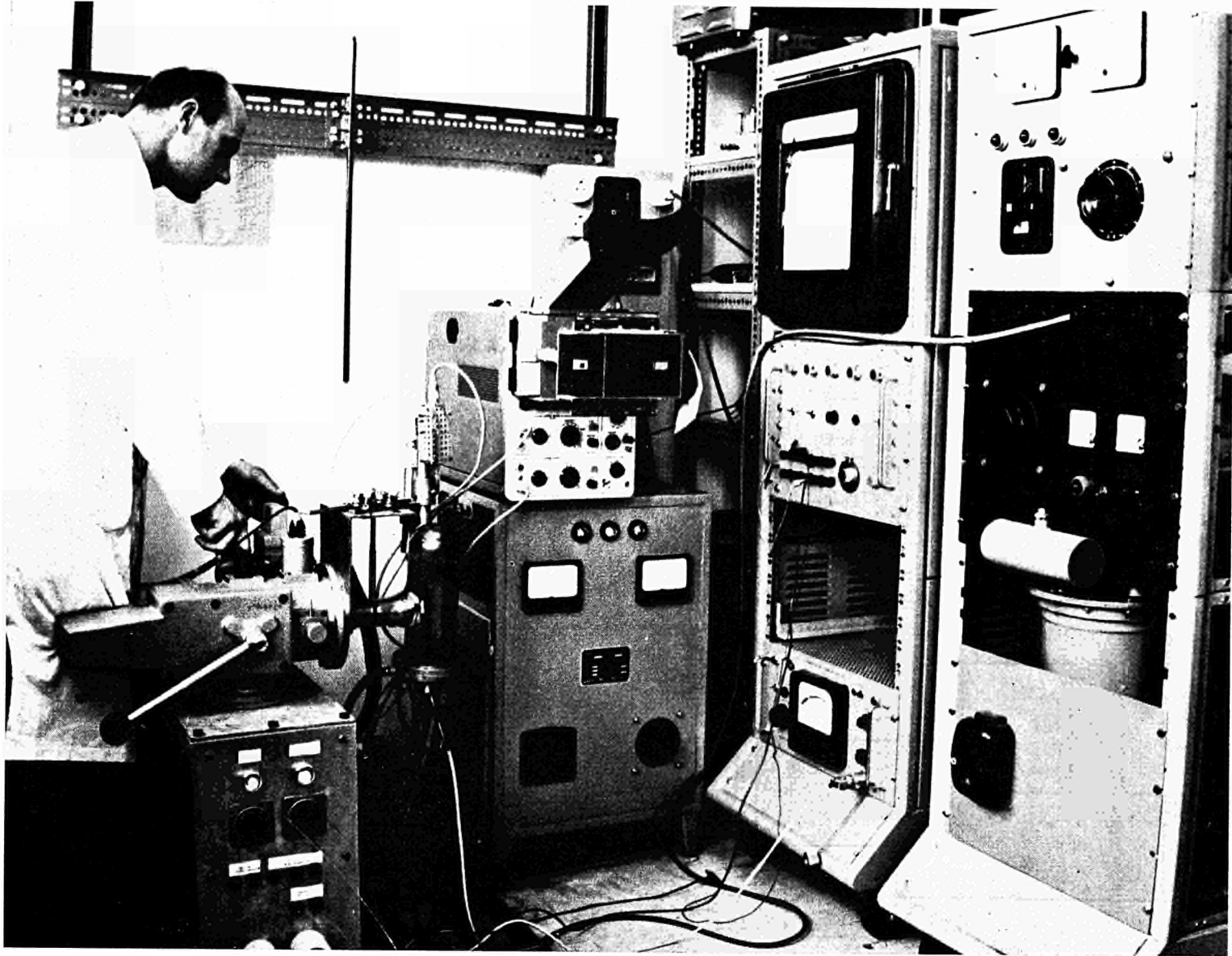
Fig. 3 — Thermal Diffusivity Apparatus
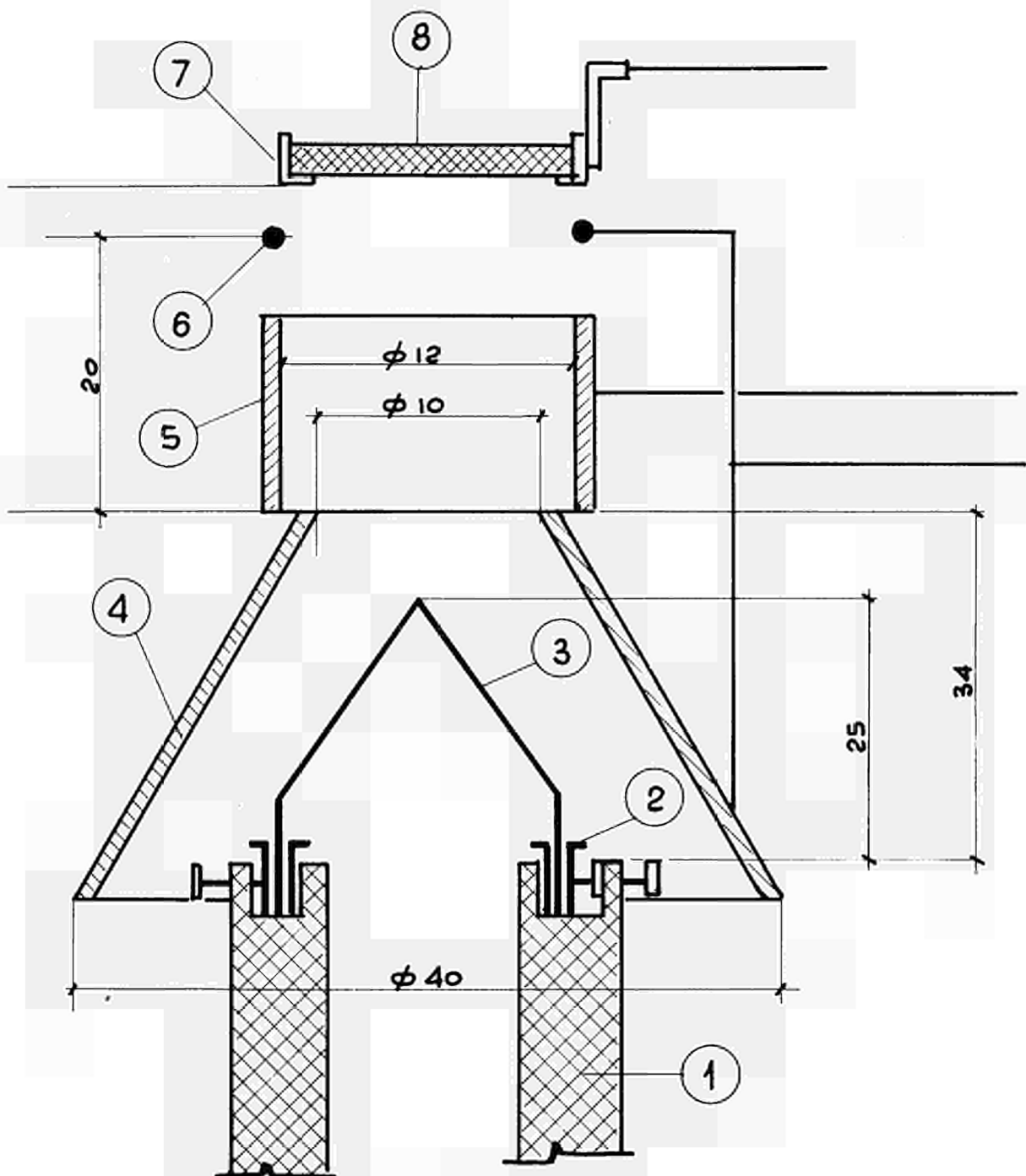
Fig. 4 — Electron gun

1. Copper filament leads 4 mm dia
2. Molybdenum filament holders
3. 36 mm thoriated tungsten filament 5 cm long
4. Modulating electrode
5. Eletrostatic lens
6. Suppressor electrode
7. Sample holder
8. UC sample
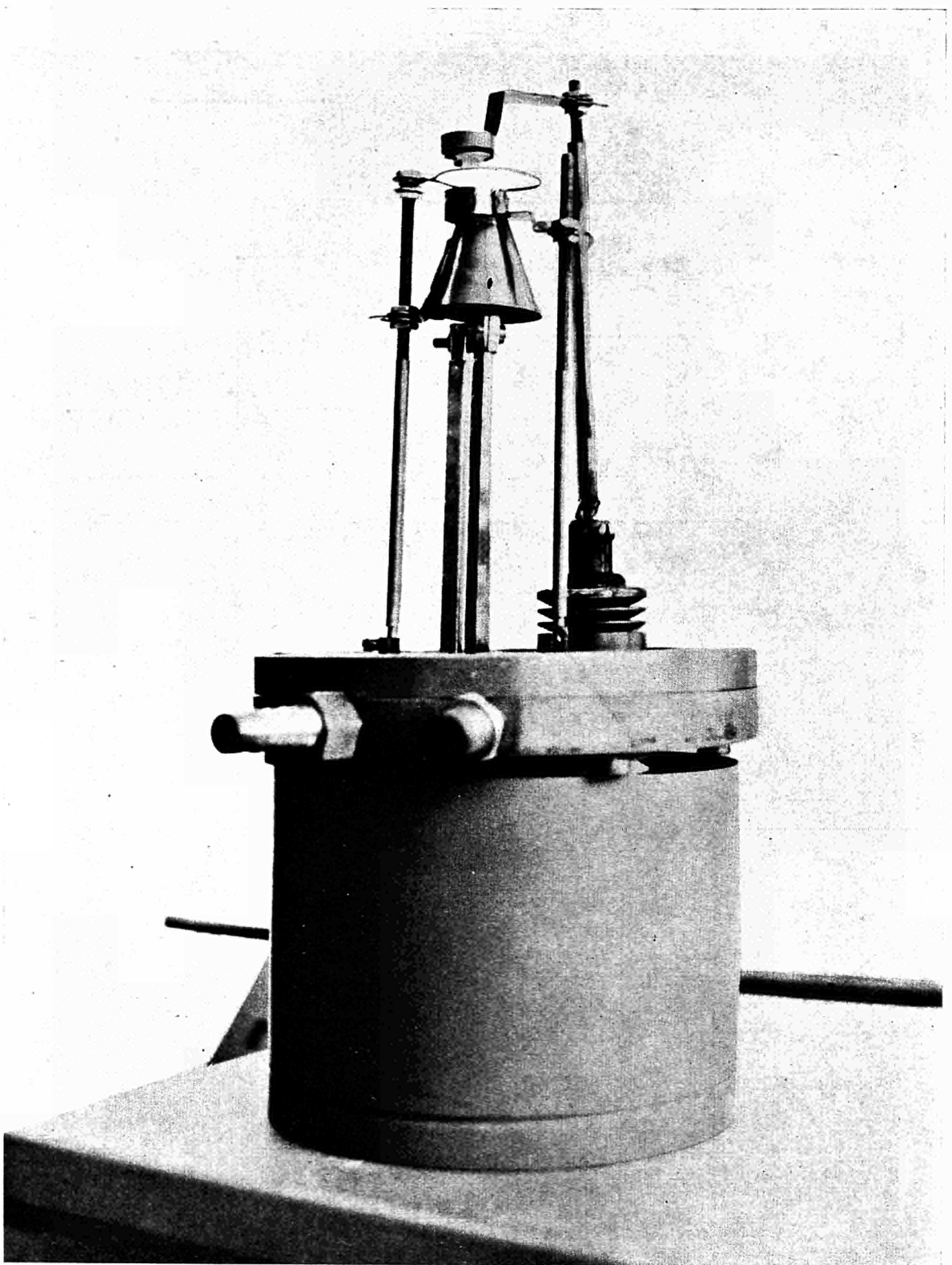
Fig. 5 — Electron gun

A thoriated tungsten filament behaves as a point source. Electrode (^{4}) is used both for focusing the beam and for modulating the beam current. It is generally operated with a fixed negative bias of -80 V on which a modulation is superposed with a maximum amplitude of 150 V. Electrode (^{5}) is a nickel cylinder biased at $+2500$ V to cause a slight convergence of the beam. Suppressor electrode (^{6}) is a molybdenum wire fit to prevent overheating and melting of sample holder (^{7}). It is electrically connected to electrode (^{4}).

The system as described resulted in a perveance of about 1.4×10^{-7} amp x volt$^{-3/2}$ and an amplification factor 50 to 100 when operated with an accelerating voltage of 5 KV and a filament heating power of 60 W.

The electron spot is fairly uniform and covers the whole target. Some filament sputtering, especially when vacuum is not better than 10^{-5} blackens the vacuum jar and causes shift in the absolute measurements of radiation without affecting the linearity of response of the photodiodes.

4.2 — Power supplies

We used an unstabilized selenium rectifier liable to give up to 20 V and 50 A to heat the filaments. A conventional G.M. power supply was used for the lens (max. 3000 V 10 ma). As to the accelerating DC supply, nothing suitable was found on the market and we built a 10 KV 500 ma max. rectifier using silicium diodes (fig. 6). This unit was voluntarily overdesigned to obtain an all-purpose HT source for future use.

4.3 — Modulation

Modulation was achieved by means of a wave function generator operated in the range .01 cps. to 100 cps. If the wave shape was to be a single pulse, a variable delay circuit was inserted between the oscilloscope trigger and the wave generator. This delay circuit provided us with a reference line for intensities measured on the oscilloscope.

4.4 — Phase analysis

Phase lags were determined with three different systems :

— Nyquist plots were made using a Solartron Resolved Component Indicator which indicated values for the component in phase and at 90 degrees to the modulating signal. Unfortunately, at frequencies below 5 cycles the system was too unstable to yield accurate results.

— A Tetronix 502, dual beam oscilloscope with a Polaroid camera was used to take pictures of both the modulating signal and the output with fairly reproducible results.

— A home-made analyser is currently being tested. It consists in a pulse generator, a pulse counter, a sinus wave generator and two flip-flop circuits. One flip-flop triggers the counter circuit when the modulating sinus passes by the zero reference line. The other flip-flop stops the counter when the output signal passes through the same reference line. Phase lags are read directly on the counter in degrees of angle.

4.5 — Samples

Vacuum melted UC pellets $1/2''$ dia. and one-and-half inch long were obtained from the Parsons Co. These samples were delivered in an as-cast condition and titled 4.8 wt. percent $C^{\pm}.1$.
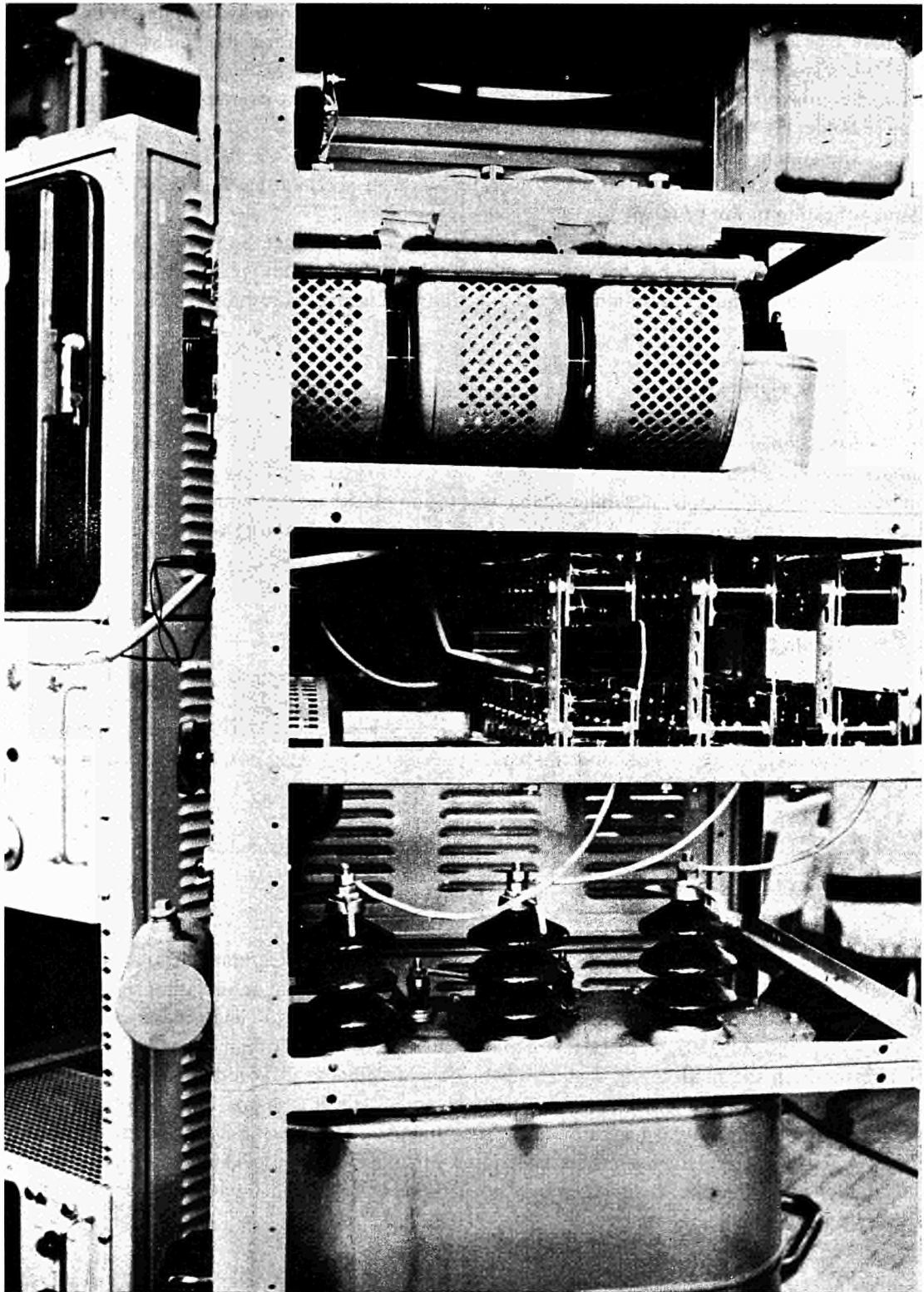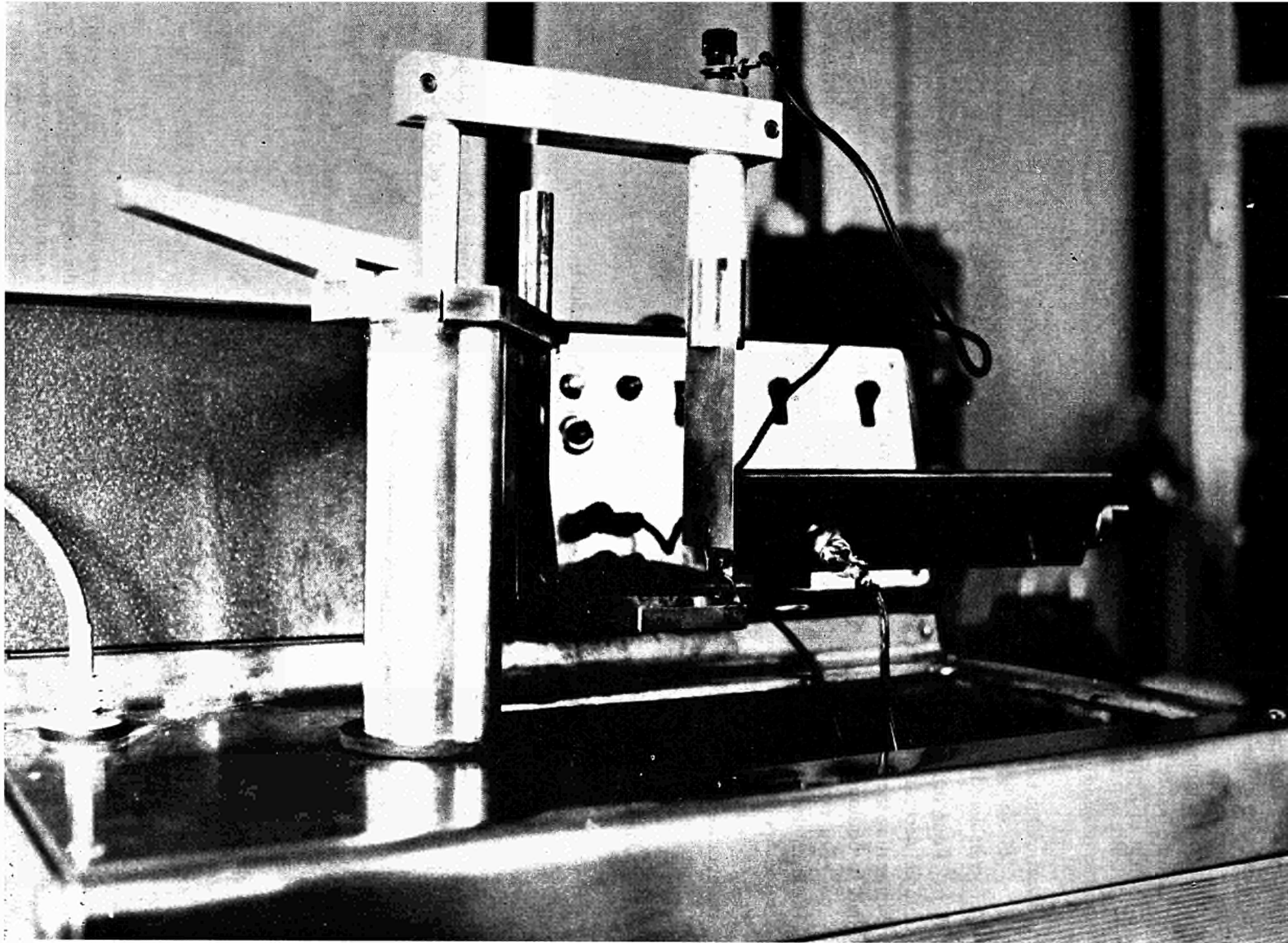
Fig. 6 — 10 KV Power supply

Fig. 7 — Cutting of UC samples

Crystallites were fairly uniform in size (10^{-2} cm) and showed tiny speckles of uncombined carbon (see fig. 1). Wafers 1 to 3 mm thick were spark-cut in a kerosene bath to prevent oxidation of the samples. The sparking electrode was a brass plate .3 mm thick (fig. 7). It underwent a linear consumption of the same order as that of the sample but left no undesired contamination on the wafer itself.

The samples were also planed by electro-sparking in kerosene, then thoroughly washed in acetone before insertion in the vacuum jar holder. At the end of this preparation UC averaged a content of 2 ppm H_2, 90 ppm O_2 and about 500 ppm N_2.

5 — EXPERIMENTAL PROCEDURES

Four different methods were tested. Whatever method was used, after mounting the sample, necessary adjustments had to be made in electrode potentials to focus the spot without overheating the holder. Albeit electrode distances were found non-critical, centering of the system had to be done accurately.

For every run a calibration was made of the photocell output vs. sample temperature. The latter was measured by means of an optical pyrometer, correcting readings with an emissivity .9 (see Appendix III).

Since darkening of the jar would prevent temperature readings at later stages of the run, a calibration was made of the power input vs. temperature.

5.1 — Amplitude method

The amplitude method makes use of relation ([2]) of Appendix II, namely

$$ln\left(\frac{\Delta t_0}{\Delta t}\right) = -\sqrt{1^2/2\alpha}\ \sqrt{w} + \text{constant}$$

frequency is varied between, say, .01 cps. and 100 cps. At each frequency the amplitudes Δt_0 and Δt_1 of the temperature fluctuations on the hind and front faces are measured on the oscilloscope trace. A plot is made of

$$\log_{10}\frac{\Delta to}{\Delta t_1}\ vs\ \sqrt{f}$$

the slope of such a plot will be

$$S = \frac{1}{2.3}\frac{d}{d\sqrt{f}}\cdot[-\sqrt{1^2/2\alpha}\ \sqrt{2\pi f}] = -\frac{1}{2,3}\sqrt{\frac{\pi l^2}{\alpha}}.$$

Thermal diffusivity is obtained as :

$$\alpha = \frac{\pi l^2}{(2,3)^2 S^2} = .59\left(\frac{1}{S}\right)^2$$

Once again we notice that since the slope alone is necessary, the absolute value of temperature fluctuations or the relative efficiency of either phototube system is not necessary. However, by means of the aforesaid temperature calibrations, a check was made to be sure that temperature fluctuations did not exceed 10°C and therefore, temperature could be considered constant in that interval.

5.2 — Output face phase shift method

This method makes use of relation ([4]), Appendix II, i.e.

$$\tan \delta_0 = \frac{b(\text{tg}B - \text{tgh}B) + 2aB\,\text{tg}B\,\text{tgh}B + 2B^2(\text{tg}B + \text{tgh}B)}{b(\text{tg}B + \text{tgh}B) + 2aB - 2B^2 \cdot (\text{tg}B - \text{tgh}B)}$$

Here again frequency is varied between .01 cps. and 100 cps. and the phase lag between electron modulation and output face temperature is measured as described in 4.5. The major uncertainty in this method is the determination of factor a. One way to overcome this difficulty is ([12]) the determination of the frequencies for which the phase lag is $\pi/4$ and $\pi/2$. The ratio of these frequencies yields a value for a.

However, a flexus in the plot δ_0 vs. $\sqrt{f}$ around $S_0 = \pi/2$ prevents a precise determination of $f(\pi/2)$. This happens especially with materials of low diffusivity ($\alpha < .1$ cm^2 sec^{-1}).

For this reason although this method was fully successful with metals, it yielded poorly reproducible results for UC.

5.3 — Differential phase shift method

This method, derived from relations (3) and (4) of Appendix II, largely eliminated the difficulties of method 5.2.

Two photocells and a mirror are used to measure simultaneously the temperature fluctuations on both faces of the wafer.

This method is fairly insensitive to the value of a (see Appendix II) and therefore requires one datum alone at a single frequency. The results obtained had very good reproducibility.

5.4 — Pulse lag method

This method is based on relation (1) Appendix II :

$$\alpha = 1.38\, l^2/\pi^2\, t_{1/2}$$

A square pulse of 10 to 25 msec duration is impressed upon the grid. A picture is taken of the oscillogram of the hind face temperature. The time $t_{1/2}$ required for temperature to attain one half of its maximum value is determined.

One requirement in this method was that in order to approximate a Dirac delta function heating, the pulse duration T must be much smaller than $t_{1/2}$, that is

$$T < \frac{1,38\, l^2}{\pi^2 2\alpha}$$

with $T = 2.5 \times 10^{-2}$ sec., $\alpha^{1/2}$ must be $\gg \dfrac{2.5 \times 10^{-2} \times \pi^2}{1.38}\,\alpha$

that is : $1 \gg .18\,\alpha^{1/2}$
with α of the order of .04 cm^2 sec^{-1} $\alpha^{1/2} \ll .2$
$1 \gg .036$ cm.

In fact, we used thicknesses between 1 and 3 mm with good results. We did not attempt to go to thicker samples because the output signal (temperature increase) and the signal-to-noise ratio would fade out.

A check was also made on one hand of the maximum temperature increase at the front face (to avoid melting or phase changes) and on the other hand the temperature increase on the hind face, to make it negligible as compared with operating temperatures. The temperature history at distance x from the surface due to a pulse of energy $f(t)$ is given by

$$T(x, t) = \frac{1}{DC(\pi\alpha)^{1/2}} \int_0^9 \frac{f(t-z) \exp(-x^2/4 \cdot z)dz}{z^{1/2}}$$

where D = density

C = specific heat

α = diffusivity

With a square pulse of duration a and height h

$$f(t) \quad \begin{aligned} &= h \quad \text{for } 0 < t < a \\ &= 0 \quad \quad t > a \end{aligned}$$

$$T(0, t) = \frac{1}{DCa(\pi\alpha)^{1/2}} \int \frac{f(t-z)dz}{z^{1/2}} = \frac{2h}{DC(\pi\alpha)^{1/2}} [\sqrt{t} - \sqrt{t-a}$$

the total pulse energy is $E = ah$, therefore

$$T(0, t) = \frac{2E}{DCa(\pi\alpha)^{1/2}} (\sqrt{t} - \sqrt{t-a})$$

Using the measured static characteristics of the experimental arrangement with an acceleration potential 3 KV, $a = 25 \times 10^{-3}$ sec a pulse height 150 V, the pulse energy is calculated to be 2.55 joule/cm^2; therefore, with $D = 3.5$, $C = .2$ joule/g°C, $\alpha = .05$ cm^2 sec^{-1}

$$T(0, t) = 173 (\sqrt{t} - \sqrt{t - .025})$$

which has a maximum at $t = .025$ sec equal to 27.3°C. This very low temperature increase guarantees that no melting or phase change will occur.

As to the hind face, its maximum temperature raise is given by

$$\Delta T \frac{E}{1 \times DC} \quad \text{with } E = 2.25 \text{ joule/cm}^2, 1 = .3 \text{ cm}$$
$$D \text{ and } C \text{ as above}$$

$$\Delta T = \frac{2.55}{3 \times 13.5 \times .2} = 3.15°C$$

This is in fact the temperature variation on which we currently based our measurements in this method. Reproducibility was very good.

6 — RESULTS

6.1 — Calibration runs

No reliable ceramic material with known thermal diffusivity between 1000 and 2000°K was available. For this reason, calibration runs were made using Nickel, Molybdenum and Niobium samples with the following results :
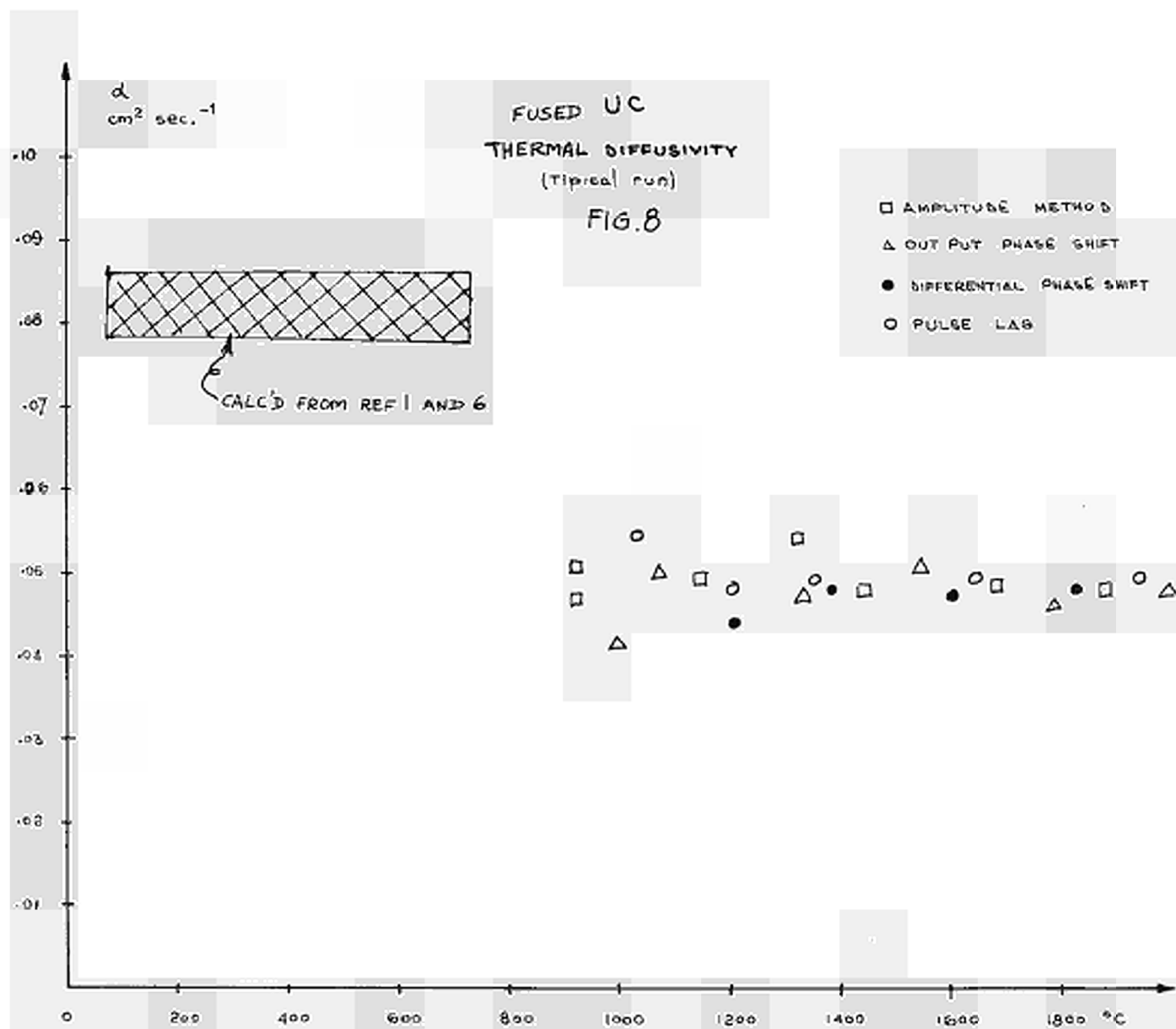
Fig. 8 — Fused UC thermal diffusivity (tipical run)

Temperature °C	Material	Thermal Diffusivity cm^2 sec^{-1}	
		Measured	Calc'd from published data ([16])
1200	Nickel	.046± .005	.048
1200	Molybdenum	.307± .010	.302
1750	Molybdenum	.200± .025	.230
1500	Niobium	.266± .025	.247

The value of the standard deviation is based on about 10 measurements for each point, repeated with the four methods described. A xi square test showed a reliable stochastic spread of results.

6.2 — Uranium carbide

About one hundred independent measurements have been performed so far on about ten different samples, using all four methods. Temperature was kept in the range 1100 to 1700°C. Results show that the thermal diffusivity of UC in this range is practically constant at a value .049± .004 cm^2 sec^{-1} (fig. 8).

The main source of error was the disuniformity of the sample thickness. In fact, the standard deviation in the measurements can well be attributed to this factor alone.

The calculation of thermal conductivity is given in Appendix III.

APPENDIX I

Transfer function of hollow cylinder

Assuming a hollow cylinder long enough to neglect radiation from the inner surface and thin enough to treat it in slab approximation, the usual Fourier equation

$$\alpha \Delta^2 T = \frac{\partial T}{\partial t} \tag{1}$$

is to be solved with boundary conditions

$$\frac{\delta T}{\delta x} = R \quad \text{in } wt \quad \text{at } x = 0$$

$$\frac{\delta T}{\delta x} = ST \qquad x = 1$$

where $R = \dfrac{-Q}{K} \quad S = \dfrac{-A}{K}$

α = thermal diffusivity
A = radiation coefficient = $4\sigma \varepsilon T^3$
Q = power modulation amplitude
l = sample thickness.

Using a solution $T = $ imaginary part of $u(x)e^{iwt} = I_m[u(x)e^{iwt}]$ equation (1) becomes

$$U'' - i\frac{w}{\alpha} u = 0$$

and $\quad u = A e^{ax} + B e^{-ax}$

where $\quad a = \sqrt{\dfrac{w}{2\alpha}} (1 + i) = (1 + i)$

if $\quad T = I_m (W)$
then $\quad W = (A e^{ax} + B e^{-ax}) e^{iwt} \tag{2}$

Boundary conditions lead to

$I_m[a(A - B)e^{iwt}] = R \sin wt = I_m[Re^{iwt}]$
or $A(A - B) = R \tag{3}$
and $SI_m[A e^{al} + B e^{-al}] e^{iwt} = ST = I_m [a(Ae^{al} - Be^{-al})e^{iwt}]$
or $a (Ae^{al} - Be^{-al}) = S(Ae^{al} + Be^{-al}) \tag{4}$

Combining (3) and (4)

$$A = \frac{\begin{vmatrix} R & -a \\ 0 & -(a+S)e^{-al} \end{vmatrix}}{\begin{vmatrix} a & -A \\ (a - S)e^{al} & -(a+S)e^{-al} \end{vmatrix}} \qquad B = \frac{\begin{vmatrix} a & R \\ (a - S)e^{al} & 0 \end{vmatrix}}{\begin{vmatrix} a & -a \\ (a - S)e^{al} & -(a+S)e^{-al} \end{vmatrix}}$$

Substituting in (2) and taking the imaginary part we obtain an analytical expression for T of the type

$$T = X \cos wt + Y \sin wt$$

The ratio $\dfrac{Y}{X}$ gives the phase lag which will be $\delta =$

$$\tan^{-1} \left[\frac{\cos a \sin ha + \sin a \cos ha - S \sin a \cos ha}{\sin a \cos ha - \cos a \sin ha + S \cos a \cos ha} \right]$$

APPENDIX II

Transfer functions in a plane geometry

This case has been extensively treated elsewhere ([11], [12], [13], [14], [15]). We shall, however, report the results which we used currently.

Pulse input

If a pulse of heat is applied on one face a slab of thickness l temperature history at the rear face will be

$$T = T_0 + \Delta T \left[1 + 2 \sum_{n=1}^{\infty} (-1)^n \exp \left(- \frac{\pi^2 n^2}{l^2} \alpha t \right) \right]$$

where T_0 i the initial temperature and ΔT is the maximum temperature raise.

For $T = T_0 + \Delta \frac{1}{2} \pi^2 \alpha t / l^2 = 1.38$ then $\alpha = 1.38 \, l^2 / \pi^2 \, t$. (1)

where t is the time elapsed until temperature has reached half of its maximum value.

Sine input

Using a sine wave with frequency $f = \frac{w}{2\pi}$ to modulate input power and calling ΔT_0 and ΔT_1 the amplitudes of temperature fluctuations on the hind and front faces respectively, it can be shown that

$$ln \left(\frac{\Delta T_0}{\Delta T_1} \right) = - \sqrt{l^2/2} \; \sqrt{w} + \text{constant}$$

provided the frequency is high enough to enable higher armonics to fade out.

On the other hand, the phase relations are ([12])

$$\tan \delta_1 = \frac{2 B^3 Q_1 + 2 B^2 a Q_2 / (1 + r) + 6 B Q_3 / r}{2 a B^2 Q_0 + b(1 + 2r) B Q_1 / r + ab Q_2 / (1 + r) + 2 B^3 Q_3}$$ (3)

and

$$\tan \delta_s = \frac{b(\text{tg} B - \text{tg} bB) + 2aB \, \text{tg} B \, \text{tg} hB + 2 B^2 (\text{tg} B + \text{tg} bB)}{b(\text{tg} B + \text{tg} bB) + 2aB - 2 B^2 (\text{tg} B - \text{tg} hB)}$$ (4)

where δ_0 = phase shift between beam modulation and output face temperature

δ_1 = phase shift between beam modulation and input face temperature

α = thermal diffusivity

$$a = l \left[\left(\frac{1}{K} \frac{\partial Q}{\partial T} \right)_{T=T_0} \cdot \left(\frac{1}{K} \frac{\partial Q}{\partial T} \right)_{T=T_1} \right]$$

$$b = l^2 \left[\left(\frac{1}{K} \frac{\partial Q}{\partial T} \right)_{T=T_0} \cdot \left(\frac{1}{K} \frac{\partial Q}{\partial T} \right)_{T=T_1} \right]$$

$B = l \sqrt{w/2\alpha}$

$Q_0 = \cos h^2 B \cos^2 B + \sin h^2 B \sin^2 B$

$Q_1 = \cos h B \sin bB + \sin bB + \cos B \sin B$

$Q_2 = \cos h^2 B \sin^2 B + \sin h^2 B \cos^2 B$

$Q_3 = \cos hB \sin hB - \cos B \sin B$

For frequencies high enough both δ_1 and δ_0 tend to increase linearly with B, i.e. with the square root of frequency. However, while δ_0 is a monotonic function, δ_1 is not, and therefore is less susceptible of yielding simple measurement techniques. In fact, $\delta_0 - \delta_1$ is the most useful datum, since with an uncertainty on the value of a as high as $.05 \leqslant a \leqslant .5$, the error on B calculated from $\delta_0 - \delta_1$ is less than 5% and the error on diffusivity no more than 10%.

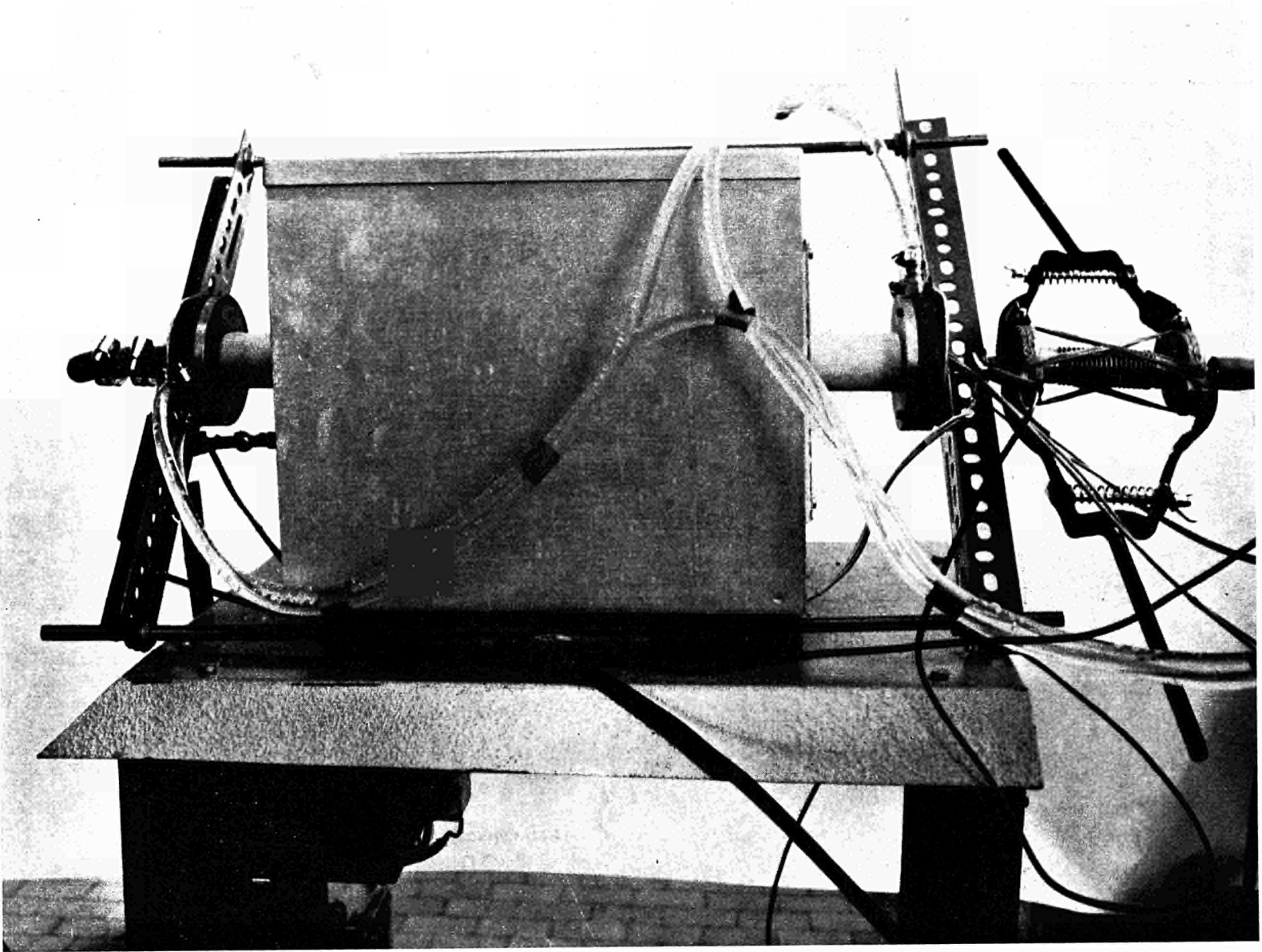Fig. 9 — UC electrical resistivity
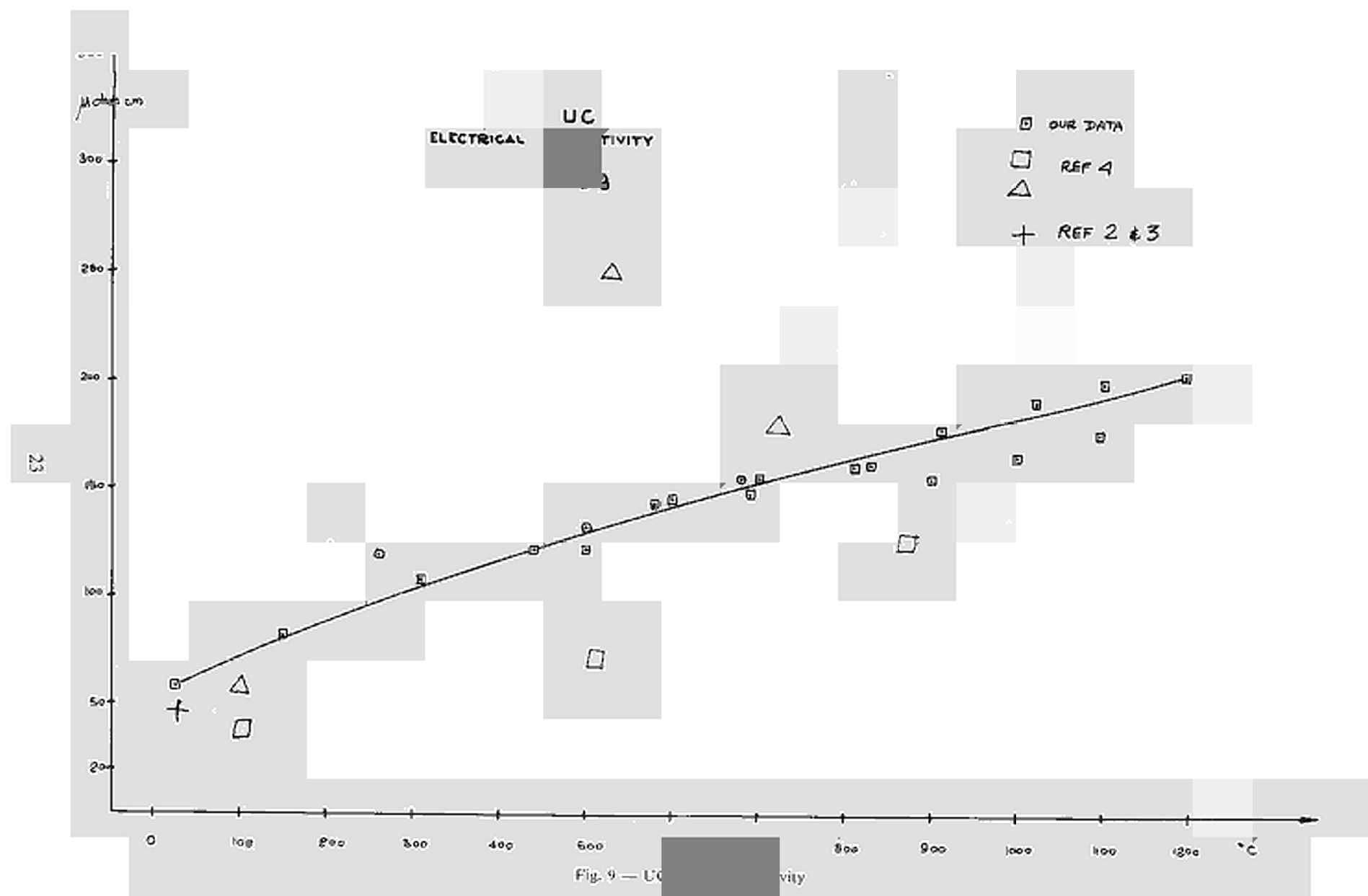
Fig. 10 — High temperature electrical resistivity assembly

24

APPENDIX III

Determination of other physical constants

In the course of the thermal diffusivity measurements, other physical properties were determined by direct measurements in the same assembly or in specially made assemblies.

Emissivity

The slope of the temperature vs. power input curve to the UC wafers yielded a value for thermal diffusivity, namely $.91 \pm .005$ for $.65\,\mu$ in good agreement with previously published data [17] with no measurable variation between 1000 and 2000 °K.

Thermal conductivity

This property can be obtained from

$$K = \alpha\, C \varrho$$

with $C = .127 + .0476 \times 10^{-3}\, T\, \dfrac{j}{g\,°C}$ (T in °K) [18]

and $\varrho = 13.6$

between 1000 and 2000 °K we shall have a near-constant value of $K = .12\ W\,\text{cm}^{-1}\,°C^{-1}$ which may be accounted for by electron transport alone (see section 2).

Electrical conductivity

Two assemblies were used to determine this property. One operating at room temperature is of conventional design and is shown in fig. 11. The other required an inert atmosphere for high temperature runs. A silica refractory tube with an Argon flow allowed measurements with good reproductibility (fig. 10).

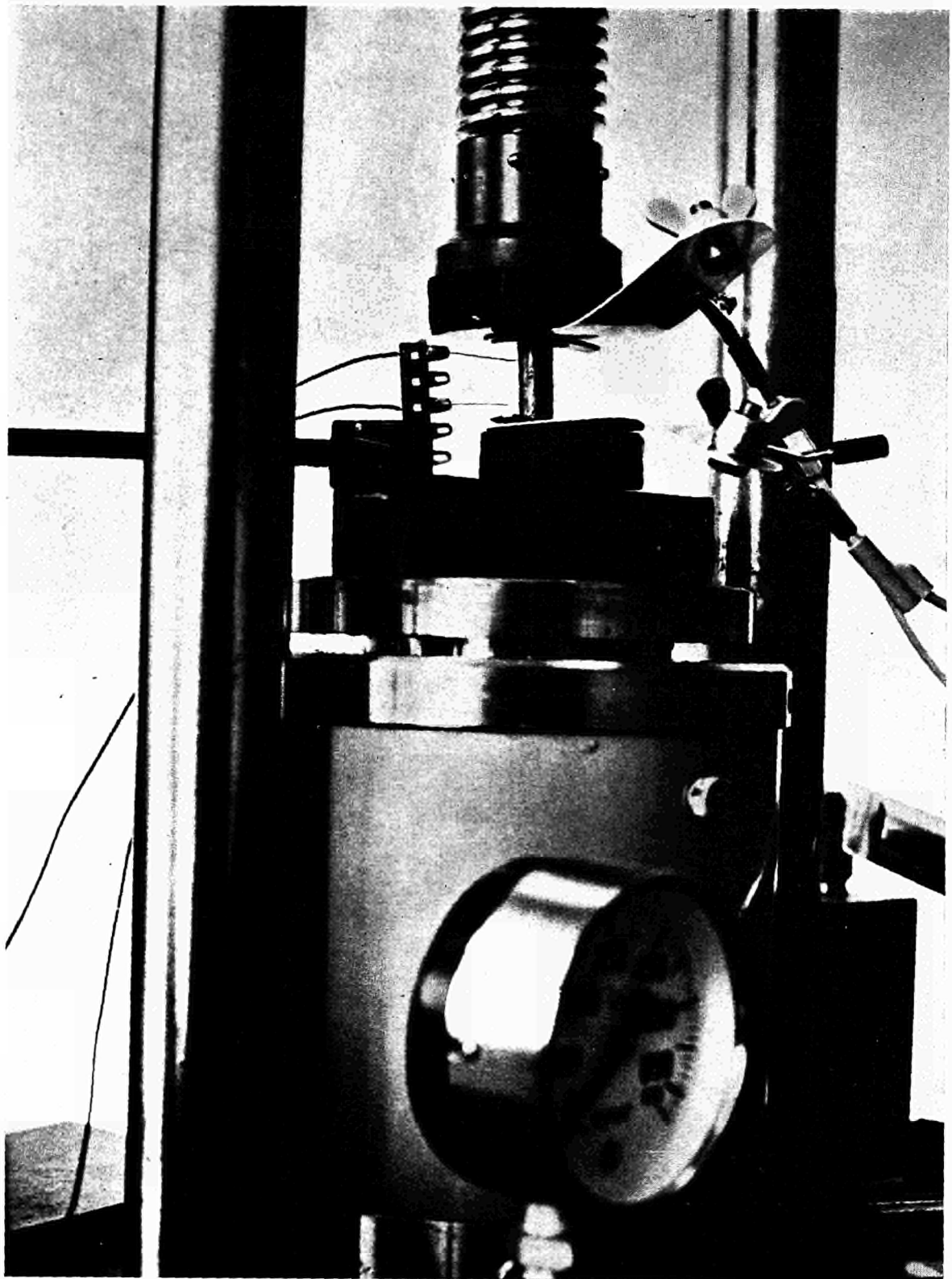These results are consistent with other published data [2,3].

25

Fig. 11 — Room temperature electrical resistivity measurement

REFERENCES

(1) A.C. SECREST Jr., et al. : "Preparation and Properties of Uranium Monocarbide Castings" BMI-1309 (Jan. 2, 1959).

(2) Progress Relating to Civilian Applications During June, 1959, BMI-1357.

(3) Progress Relating to Civilian Applications During May, 1959, BMI-1346.

(4) A. ACCARY, R. CAILLAT : "Development of Ceramic Fuel Elements in France" from "Nuclear Fuel Elements – Rheinold Publishing Corp., N. Y. (1959).

(5) R.M. POWERS, et al.: The effect of solid solution additions on the thermal conductivity of UO₂", SCNC – 317 (Nov., 1960).

(6) A. BOETTCHER and G. SCHNEIDER : "Some properties of Uranium Monocarbide", A/Conf. 15/P/964.

(7) O. KUBACHEWSKI and E.L. EVANS : "Metallurgical Thermochemistry", John Wiley and Sons, Inc., N. Y. (1958).

(8) E. GENZEL, Z. Physik, 135, 177 (1953).

(9) M. GUTLER, et al. : "Thermal Conductivity of Reactor Materials", GA-1939 (Jan. 30, 1961).

(10) W.D. KINGERY : "The thermal Conductivity of Ceramic Dielectrics" from Progress in Ceramic Science, 2, 182 (1962).

(11) H.S. CARSLAW and J.C. JAEGER : "Conduction of heat in solids", 2nd edition Oxford at Clarendon Press, (1959).

(12) R.D. COWAN : "Proposed method of measuring thermal diffusivity at high temperature", LA-2460, Nov., 1960.

(13) E.L. WOISARD : "Pulsed method for the Measurement of Thermal Diffusivity of Metals", Journ. of Applied Physics, 32, Jan., 1961.

(14) W.J. PARKER, et al. : "Flash method of determining Thermal Diffusivity, Heat Capacity and Thermal Conductivity, J. of Appl. Physics, 32, 1679, Sept., 1961.

(15) J.B.J. FOURIER : "Extrait d'un Mémoire sur le refroidissement du globe terrestre", Bull. Sci. de la Société Philomathique de Paris, (1820).

(16) R.P. TYPE, "Preliminary measurements on the thermal and electrical conductivities of Molybdenum, Niobium, Tantalium and Tungsten", from "Niobium, Ta, Mo, W", edited by A.G. Quarrel-Elsevier, 1961.

(17) G.A. HAAS and J.T. JENSEN, Jr. : "Thermionic Properties of UC", Journal of Appl. Physics, 31, 1231, July, 1960.

(18) A.B. TRIPLER, Jr., et al.: "Further Studies of Sintered Refractory Uranium Compounds", BMI-1313 (Jan., 27, 1959).